Observation of Multipactor in an Alumina-Based Dielectric-Loaded Accelerating Structure

J. G. Power,[1] W. Gai,[1] S. H. Gold,[2] A. K. Kinkead,[3] R. Konecny,[1] C. Jing,[1] W. Liu,[1] and Z. Yusof[1]
[1]*High Energy Physics Division, Argonne National Laboratory, Argonne, Illinois 60439, USA*
[2]*Plasma Physics Division, Naval Research Laboratory, Washington, D.C. 20375, USA*
[3]*LET Corporation, Washington, D.C. 20007, USA*
(Received 12 September 2003; published 22 April 2004)

We report a new regime of single-surface multipactor that was observed during high-power testing of an 11.424-GHz alumina-based dielectric-loaded accelerating structure. Previous experimental observations of single-surface multipactor on a dielectric occurred in cases for which the rf electric field was tangential and the rf power flow was normal to the dielectric surface (such as on rf windows) and found that the fraction of power absorbed at saturation is ~1%, independent of the incident power. In this new regime, in which strong normal and tangential rf electric fields are present and the power flow is parallel to the surface, the fraction of power absorbed at saturation is an increasing function of the incident power, and more than half of the incident power can be absorbed. A simple model is presented to explain the experimental results.

DOI: 10.1103/PhysRevLett.92.164801 PACS numbers: 41.75.Lx, 29.17.+w, 52.80.Pi, 84.90.+a

The development of new rf accelerating structures that are capable of producing gradients in excess of 100 MV/m is currently an active area of basic accelerator research, with applications ranging from medical accelerators to high-energy physics [1]. While current traveling-wave electron linear accelerators use disk-loaded metal structures to reduce the phase velocity of the rf wave to match the particle velocity, other concepts are under investigation. One class of structures that looks particularly promising is the dielectric-loaded accelerator (DLA), in which a uniform dielectric-lined metal tube replaces the metal disk-loaded structure [2,3]. In this Letter, we report on the observation of a multipactor phenomenon that can occur during high-power operation of such structures and absorb a significant fraction of the incident power.

Multipactor is an electron multiplication process that can take place on surfaces exposed to rf fields in vacuum. Multiplication occurs when an electron gains energy from the rf field and strikes the surface with an impact energy K in an energy range with secondary electron yield δ (the ratio of electrons emitted from the surface to electrons impacting the surface) greater than 1 [4]. Most previous observations and modeling of multipactor fall into two groups: (i) resonant two-surface multipactor across a metallic gap (e.g., an rf cavity), where the rf electric field is normal to the surface [5,6], and (ii) single-surface multipactor on a planar dielectric surface (e.g., an rf window), where the power flow is normal to the surface and the rf electric field is tangential [7–10]. In the latter case, multipactor typically saturates with the absorption of the order of 1% of the incident power, and, once the multipactor threshold is exceeded, the fraction of power absorbed is independent of the incident power.

However, multipactor on the interior of a dielectric tube, due to the radial and axial electric fields of the propagating TM_{01} mode, is an example of the general problem of single-surface multipactor on a dielectric surface in the presence of both normal and tangential rf fields. Valfells *et al.* [11] made a theoretical study of multipactor on dielectric windows for this general case but considered only the average secondary yield of a uniform phase distribution of secondary electrons, in order to determine the conditions for multipactor saturation. Our results show that when the normal component of the rf electric field is large, a new regime of multipactor is entered where electrons emitted only from a narrow band of emission phases contribute to multipactor at saturation. The consequences of our results are explained below.

These observations were made during high-power tests of DLA structures using the 11.424-GHz magnicon facility at the Naval Research Laboratory [12,13]. Power from the magnicon is first coupled from the rectangular to the cylindrical copper waveguide with a $TE_{10} - TM_{01}$ mode converter [14] and then into the structure (Fig. 1), which consists of a uniform alumina-lined copper tube, with tapered transitions at either end. The TM_{01} rf fields within the central vacuum region ($r < a$) are given by

$$E_z = E_{\mathrm{rf}} I_0(k_r r)\cos(\omega t - k_z z), \tag{1}$$

$$E_r = E_{\mathrm{rf}}\left(\frac{k_z}{k_r}\right) I_1(k_r r)\sin(\omega t - k_z z), \tag{2}$$

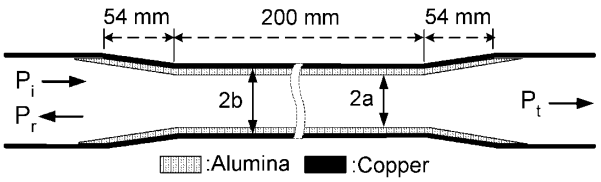

FIG. 1. Cross section of the cylindrical DLA structure. (a = 5 mm; b = 7.185 mm).

 0031-9007/04/92(16)/164801(4)$22.50

$$H_\varphi = E_r/Z_{\mathrm{TM}}, \quad (3)$$

where E_{rf} is the rf field amplitude, k_r and k_z are the radial and longitudinal wave numbers, respectively, ω is the angular frequency, $I_n(x)$ is the modified Bessel function of the first kind, and Z_{TM} is the impedance of the TM wave.

Following bakeout and rf conditioning, the incident (P_i), reflected (P_r), and transmitted (P_t) rf powers were measured with directional couplers as P_i was varied over the range of 5 kW to 5 MW in 150 ns FWHM pulses, corresponding to E_{rf} in the alumina DLA structure of 25 kV/m to 8 MV/m. The measured power transmission and reflection coefficients (P_t/P_i and P_r/P_i) are shown in Fig. 2(a). Their values were constant and consistent with low-power bench-top measurements ($P_t/P_i \approx 75\%$ and $P_r/P_i \approx 0.5\%$), over the range of ~5 to 80 kW. However, at higher powers, P_t/P_i was found to decrease monotonically as a function of P_i, without a corresponding increase in P_r/P_i. In other words, an increasing fraction of the incident power was unaccounted for by transmission, reflection, or the attenuation expected in the structure. We refer to this additional lost power as the *missing power* P_m. At the highest incident power $P_i =$ 4.7 MW, $P_t = 1.2$ MW, the expected loss due to structure attenuation was 1.2 MW, and P_r was 65 kW. In this case, P_m was 2.3 MW, approximately one-half of P_i. Note that this effect was fully reversible, and no rf breakdown or permanent change to the DLA structure was observed.

Coincident with the missing power, light emission was observed from the surface of the alumina, with intensity proportional to the missing rf power [Fig. 2(b)]. The inset in Fig. 2(b) shows two images of this light that were taken with a charge-coupled device (CCD) camera. In 2(c), the camera was aligned with the axis of the dielectric tube, so that only light emission from the tapered transition section (Fig. 1) at the end of the alumina DLA structure is clearly visible, with the dark central region corresponding to the hole through the center of the structure. In Fig. 2(d), the camera was pointed slightly off axis, so that light emission from the wall of the uniform accelerating section is also visible. The difference in apparent brightness is due in part to different aperture settings on the CCD camera. The luminescence and the missing power suggested the presence of multipactor in the structure — similar to the phenomenon that is observed on dielectric rf windows [7–11].

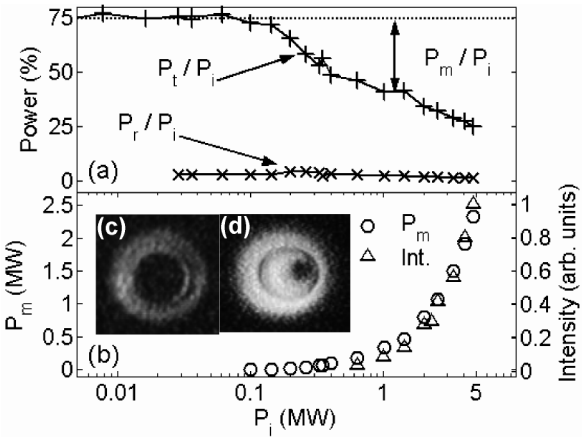

FIG. 2. Measured values of (a) the transmission and reflection coefficients and (b) the missing power and the time-integrated light intensity as a function of incident power. (c),(d) Images of light observed during the high-power test of the alumina DLA structure.

Figure 3 shows experimental traces of incident, transmitted, and reflected power at an incident power of 1.3 MW. In the right-hand set of traces, a 100-G horseshoe magnet has been placed near the structure. The transverse magnetic field clearly affects the leading edge of the transmitted power curve, suggesting that low energy electrons are involved in this process (as is expected for multipactor), but otherwise has no significant effect on the transmitted power. Particularly in the second case, there is remarkable similarity between the three waveforms, suggesting that the process that absorbs rf power corresponds to the instantaneous rf power. This is consistent with the multipactor process, which can exponentiate on a time scale on the order of the rf period (~90 ps) and thus readily track an rf pulse with a rise time and a fall time of ~100 ns. The shape of the rising and falling portions of the waveforms in Fig. 3(b) are almost identical, suggesting that there is no buildup of ions during the rf pulse.

Simulations were made to model multipactor onset and saturation in the alumina DLA structure. The multipactor model computes electron trajectories inside the structure under the influence of the dc and rf fields. The dc field E_{dc} arises from the radial space-charge field of a thin cylindrical shell of secondaries [Fig. 4(a)] with trajectories near the surface of the dielectric. (Because of symmetry, the surface charge on the dielectric does not contribute to the dc field in the vacuum region.) The assumption of a thin shell distribution of electrons near saturation is

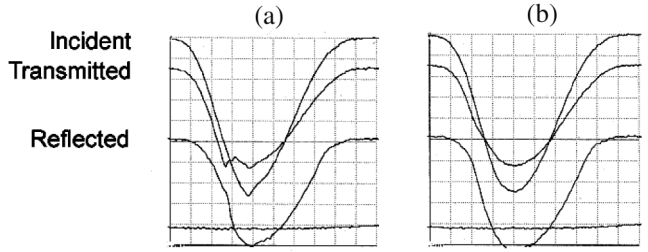

FIG. 3. Traces of incident, transmitted, and reflected microwave signals from the alumina DLA structure, with no magnet (a) and with a permanent magnet in vicinity of input tapered section (b). The vertical scales of the three traces are different from each other, but the same for the left and right sets. The horizontal time scale is 50 ns/div.

justified since the computed trajectories stay near the surface. The comparatively low velocity of the secondary electrons allows us to neglect the azimuthal rf magnetic fields, permitting us to reduce the problem to 2D [Fig. 4(b)], in which the equations of motion near the surface become

$$m\ddot{z} = -eE_{\mathrm{rf}}\cos(\omega t - k_z z + \theta), \tag{4}$$

$$m\ddot{r} = -eE_{\mathrm{dc}} - eE_{\mathrm{rf}}\left(\frac{\pi a}{\lambda_z}\right)\sin(\omega t - k_z z + \theta), \tag{5}$$

where the dot represents differentiation with respect to time, θ is the rf phase at the instant of emission, $\lambda_z = 2.6$ cm is the guide wavelength, and we have used $I_0(k_r r) \cong 1$ throughout the vacuum region and $\frac{k_z}{k_r} I_1(k_r r) \cong (\frac{\pi a}{\lambda_z})$ near the surface. Note that the coordinate r in Eq. (5) is defined so that $r = 0$ corresponds to the surface of the dielectric. As shown in Fig. 4(b), the electrons are emitted from the surface with emission angle ϕ_0 and emission velocity $v_0 = \sqrt{2e_0/m}$, where e_0 is the emission energy and m is the mass of the electron.

Multipactor growth begins when electrons strike the surface with an impact energy K greater than the minimum energy for which δ is greater than 1. This energy threshold, e_1, is known as the first crossover point of the secondary electron emission curve [4] and was estimated by calculating the energy gained at impact within one rf period by electrons launched from rest ($e_0 = 0$), over all possible emission phases ($0^0 < \theta < 360^0$), as a function of the rf field amplitude E_{rf}, with E_{dc} set to 0 (i.e., no initial space-charge cloud). Solving Eqs. (4) and (5) with $E_{\mathrm{rf}} \approx 1$ MV/m (Fig. 1, power loss at $P_i \approx 80$ kW) gives that the maximum impact energy is $K \approx 60$ eV, which falls within the expected range for alumina: $3 < e_1 < 300$ eV [7,8].

Once the multipactor threshold is crossed ($K > e_1$), the number of electrons inside the DLA structure will rapidly increase until saturation, which occurs when the space-charge field due to the secondary electrons becomes large enough to suppress further electron multiplication. To simplify our model, we assume that secondary electrons are emitted normal to the surface [$\phi_0 = \pi/2$ in Fig. 4(b)]; are monoenergetic, with energy e_0; and experience a space-charge field E_{dc} due to the total number of electrons in the structure is not adjusted to take into account the instantaneous radius of the electron.

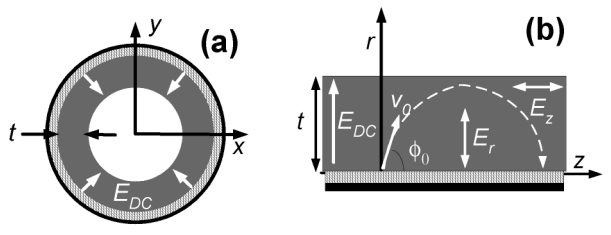

FIG. 4. Model of single-surface multipactor with both normal and tangential rf fields and normal dc field caused by an electron cloud of thickness t (shaded) in the cylindrical DLA structure. (a) End view; (b) side view.

Our simulations reveal that the saturation condition for the DLA structure is qualitatively different from that of the rf window with only a tangential electric field. In the rf window case, saturation occurs when E_{dc} has increased to a level such that the phase-averaged value of the impact energy K decreases to the first crossover energy e_1 [7,9,10]. At this point, the secondary electrons impact the surface with energy e_1, at a rate of once per hop time τ, where $\tau \propto E_{\mathrm{dc}}^{-1}$. This leads to a saturated state in which the power absorbed is *on the order of 1%*. As shown below, saturation in the DLA structure occurs when electrons fall out of synchronism with the rf, and not when K drops to e_1. In fact, K is much greater than e_1 at high values of E_{rf}, which can lead to the 50% power loss observed in the experiment.

The essential features of the saturation condition are most easily understood by temporarily setting the emission energy e_0 to 0. (Realistic values are used in the detailed simulations.) Electron trajectories were computed for a uniform distribution of emission phase angles θ. For each value of E_{rf}, E_{dc} was systematically raised from zero until saturation occurred. In this model, the trajectories are permitted to hop along the surface by the immediate emission of new electrons at the point of impact, when the rf phase permits this to occur. Trajectories that can propagate indefinitely will lead to exponentiation of the electron density, provided that $K > e_1$. Slightly below saturation, such trajectories fall within a narrow range of emission phases θ_{min} to θ_{max}, with $\tau \approx T_{\mathrm{rf}}$, the rf period. After a few hops along the surface, these trajectories undergo phase focusing until $\tau = T_{\mathrm{rf}}$. Trajectories just outside this narrow range of emission phases fall out of phase with the rf field after several hops and end when the rf phase at impact suppresses reemission. All the other trajectories either stop after their first hop or do not leave the surface at all. As E_{dc} is increased toward saturation, τ decreases, and θ_{max} approached θ_{min}. Saturation is reached when E_{dc} has increased to a value such that the duration of the longest trajectory is exactly T_{rf}. This *resonant* trajectory occurs when the sum of E_{dc} and the normal component of E_{rf} goes through zero and points into the surface, so that electrons can be accelerated outward.

Further insight can be gained by solving the equations of motion under the approximation that the k_z dependence can be ignored, since $\omega/k_z \approx c \gg \dot{z}$. Solving Eq. (5) with $e_0 = 0$ shows that the above-mentioned resonant trajectory begins at the surface with rf phase $\theta = \pi + \mathrm{Tan}^{-1}(1/\pi)$, occurs at dc field $E_{\mathrm{dc}} \approx 0.303 E_{\mathrm{rf}}(\frac{\pi a}{\lambda_z})$, and has an impact velocity $v = \frac{2\pi e E_{\mathrm{dc}}}{m\omega}$ normal to the surface. Solving Eq. (4), we see that the tangential velocity at impact is equal to its initial velocity (zero), since the trajectory lasts exactly one rf period. Thus, this regime

of multipactor is driven by the normal component of the rf field. Since electrons gain energy from the rf field and lose it in collisions with the surface, the power lost is $P = N_e K/\tau$, where N_e is the number of electrons with impact energy K striking the surface per hop time $\tau = T_{\rm rf}$. Since $N_e \propto E_{\rm dc} \propto E_{\rm rf}$ and $K \propto v^2 \propto E_{\rm rf}^2$, the absorbed power scales as $P_i^{3/2}$ for this approximation, which shows reasonable agreement with detailed modeling.

The most important consequence of this saturation condition is that the electrons impact the surface at high energy. The value of K at saturation is plotted as a function of $E_{\rm rf}^2$ in Fig. 5(a). In contrast to the case of rf window multipactor, where K at saturation would be equal to e_1 ($\approx$60 eV for the alumina tube), the predicted value of K at saturation is found to increase rapidly with increasing values of $E_{\rm rf}$ and reaches $\sim$2 keV at the highest rf fields tested in the experiment.

To check the validity of our model, we set $e_1 = 60$ eV and varied e_0 over the expected range of 1.75–6.5 eV [7,8]. To estimate N_e, we calculated the charge enclosed per unit length, $\rho_e = eN_e/L$, where L, the effective length of the alumina DLA structure, should fall between the length of the center section alone, 200 mm, and the total length of 308 mm (Fig. 1). Applying Gauss's law in cylindrical coordinates gives $\rho_e = 2\pi a \varepsilon_0 E_{\rm dc}$, where $E_{\rm dc}$ is the value of the space-charge field at saturation for a given rf field $E_{\rm rf}$. The rf field amplitude $E_{\rm rf}$ in the DLA structure was estimated from the average power in the rf tube by averaging P_i and P_t. (Shielding of the rf at the surface by the electron layer is not a factor, because the plasma frequency is below the rf frequency.) The best fit to the experiment was found by setting $e_0 = 2$ eV and $L = 250$ mm. The excellent agreement for this choice of values, as shown in Fig. 5(b), suggests that this simple model is capturing the essential physics of this multipactor process.

In conclusion, we have observed single-surface multipactor in a high-power test of an X band, alumina-based traveling-wave cylindrical DLA structure. This test was carried out at up to 5 MW incident power, corresponding to an accelerating gradient of $\sim$8 MV/m, and demonstrated, for the first time, that a DLA structure is capable of withstanding such power levels without rf breakdown. However, for incident powers above $\sim$80 kW, the attenuation of rf power within the alumina DLA structure progressively increased as a function of drive power, due to multipactor. This was accompanied by light emission from the inner surface of the alumina. At the highest power tested, approximately half of the drive power was absorbed by this process. We have developed a model that demonstrates the essential features of the experimental observations. The multipactor process is driven by the normal component of the TM_{01} rf fields that are used to accelerate electrons through the DLA structure, leading to a saturation mechanism that is considerably different and a saturated power loss that is significantly higher than for single-surface multipactor on rf windows. Because the tangential component of the electron motion is not important, it may be possible to suppress this multipactor using an axial magnetic field. However, the key to its suppression appears to be to lower the secondary emission coefficient of the dielectric surface using, for example, a thin TiN coating. As an alternative, DLA structures can be fabricated using dielectrics with values of δ lower than alumina. These approaches will be tested in future work.

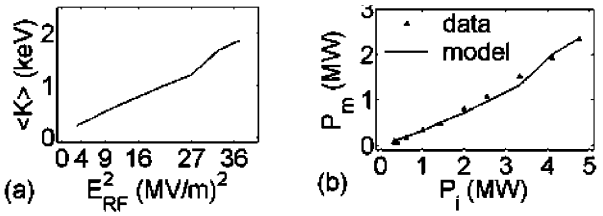

FIG. 5. (a) Predicted average impact energy at saturation vs rf field squared from the model. (b) Comparison of experimental missing power data to the model.

This work was supported by the Division of High-Energy Physics, U.S. Department of Energy and by the U.S. Office of Naval Research. We thank M. E. Conde, A. W. Fliflet, D. Lewis, Y. Y. Lau, and A. Zinovev for many useful discussions.

[1] E. C. Colby, in *Advanced Accelerator Concepts: Tenth Workshop*, edited by Christopher E. Clayton and Patrick Muggli, AIP Conf. Proc. No. 647 (AIP, 2002), p. 39.
[2] P. Zou *et al.*, Rev. Sci. Instrum. **71**, 2301 (2000).
[3] E. Chojnacki *et al.*, J. Appl. Phys. **69**, 6257 (1991).
[4] J. R. M. Vaughn, IEEE Trans. Electron Devices **36**, 1963 (1989).
[5] J. R. M. Vaughn, IEEE Trans. Electron Devices **35**, 1172 (1988).
[6] R. A. Kishek and Y. Y. Lau, Phys. Rev. Lett. **75**, 1218 (1995).
[7] L.-K. Ang *et al.*, IEEE Trans. Plasma Sci. **26**, 290 (1998).
[8] R. A. Kishek *et al.*, Phys. Rev. Lett. **80**, 193 (1998).
[9] A. Neuber *et al.*, J. Appl. Phys. **86**, 1724 (1999).
[10] A. Valfells *et al.*, IEEE Trans. Plasma Sci. **28**, 529 (2000).
[11] A. Valfells *et al.*, Phys. Plasmas **7**, 750 (2000).
[12] S. H. Gold *et al.*, in *Advanced Accelerator Concepts: Tenth Workshop* (Ref. [1]), p. 439.
[13] J. G. Power *et al.*, in *Proceedings of the 2003 Particle Accelerator Conference, Portland, OR*, edited by Joe Chew, P. Lucas, and Sara Webber (IEEE, Piscataway, NJ, 2003), p. 492.
[14] W. Liu *et al.*, in *Proceedings of the 2003 Particle Accelerator Conference, Portland, OR* (Ref. [13]), p. 1810.